

Temperature-dependent oxide removal from manganese- and iron oxide-coated soil redox bars

Kristof Dorau¹ · Samuel Papenfuß¹ · Tim Mansfeldt¹

Received: 20 February 2017 / Accepted: 14 August 2017 / Published online: 21 August 2017
© Springer-Verlag GmbH Germany 2017

Abstract

Purpose Soil temperature is a fundamental parameter affecting not only microbial activity but also manganese (Mn^{III,IV}) and iron (Fe^{III}) oxide reduction rates. The relationship between Mn^{III,IV} oxide removal from oxide-coated redox bars is missing at present. This study investigated the effect of variable soil temperatures on oxide removal by Mn^{III,IV} and Fe^{III} oxide-coated redox bars in water-saturated soil columns in the laboratory.

Materials and methods The Mn coatings contained the mineral birnessite, whereas the Fe coatings contained a mixture of ferrihydrite and goethite. Additionally, platinum (Pt) electrodes designed to measure the redox potential (E_H) were installed in the soil columns, which were filled with either a humic topsoil with an organic carbon (C_{org}) content of 85 g kg⁻¹ (pH 5.8) or a subsoil containing 2 g C_{org} kg⁻¹ (pH 7.5). Experiments were performed at 5, 15, and 25 °C.

Results and discussion Although elevated soil temperatures accelerated the decrease in E_H after water saturation in the topsoil, no E_H decreases regardless of soil temperature occurred in the subsoil. Besides soil temperature, the importance of soil organic matter as an electron donor is highlighted in this case. Complete removal of the Mn^{III,IV} oxide coating was observed after 28, 14, and 7 days in the soil columns filled with topsoil at 5, 15, and 25 °C, respectively. Along the Fe redox bars, Fe^{III} reducing conditions first appeared at 15 °C and oxide removal was enhanced at 25 °C because of lower E_H , with the preferential dissolution of ferrihydrite over goethite as revealed by

visual differences in the Fe^{III} oxide coating. Oxide removal along redox bars followed the thermodynamics of the applied minerals in the order birnessite > ferrihydrite > goethite.

Conclusions In line with Van't Hoff's rule, turnover rates of Mn^{III,IV} and Fe^{III} oxide reduction increased as a result of increased soil temperatures. Taking into account the stability lines of the designated minerals, E_H -pH conditions were in accordance with oxide removal. Soil temperature must therefore be considered a master variable when evaluating the oxide removal of redox bars employed for the monitoring of soil redox status.

Keywords Iron oxides · Manganese oxides · Microbial activity · Redox potential · Soil temperature

1 Introduction

Soils are open and porous systems composed of solids, liquids, and gases, and are involved in a continuous exchange of matter and energy with the surrounding spheres. In wetland soils, flooding or other events cause water saturation that hampers the replenishment of oxygen (O₂) from the atmosphere. Consequently, the availability of O₂ is in a transient state and is not constant over time, because heterotrophic microorganisms consume O₂ by reduction to water during the process of aerobic respiration (Glinski and Stepniewski 1985). Specialized microbes such as *Geobacter* or *Shewanella* are able to reduce tri- and tetravalent manganese (Mn^{III,IV}) and trivalent iron (Fe^{III}) oxides under the absence of more favorable terminal electron acceptors such as O₂ or nitrate (NO₃⁻) (Martin 2005). Microbial activity is sensitive to changes in soil temperature and consequently has an impact on the reduction rates of Mn^{III,IV} and Fe^{III} oxides (Lovley 1991).

Various methods are available with which to document reducing conditions in soils, ranging from cost-intensive but fully

Responsible editor: Claudio Zaccone

✉ Kristof Dorau
k.dorau@uni-koeln.de

¹ Department Geowissenschaften, Bodengeographie/Bodenkunde, Universität zu Köln, Albertus-Magnus-Platz, 50923 Köln, Germany

automated systems using platinum (Pt) electrodes and data loggers (Patrick et al. 1996; Fiedler et al. 2007), laborious, time- and sampling-intensive techniques based on the terminal electron-accepting processes approach (Chapelle et al. 1995), through to inexpensive iron metal rods that provide little insight into the temporal extent of soil reducing conditions (Owens et al. 2008). Iron oxide-coated polyvinyl chloride (PVC) tubes were introduced by Jenkinson and Franzmeier (2006) to document and monitor soil redox status via the depletion of the synthesized Fe^{III} oxide coating under soil reducing conditions. This method was later adapted using $\text{Mn}^{\text{III,IV}}$ oxides as the coating agent (Dorau and Mansfeldt 2015) to differentiate between weakly (E_{H} 300 to 100 mV at pH 7; range of $\text{Mn}^{\text{III,IV}}$ oxide reduction) and moderately reducing conditions (E_{H} 100 to – 100 mV at pH 7; range of ferrihydrite reduction) in the field. In waterlogged soils, whereas the critical value for the onset of $\text{Mn}^{\text{III,IV}}$ oxide reduction is 300 to 200 mV (Gotoh and Patrick 1972), the transformation of Fe^{III} oxides starts at 100 mV under neutral soil reaction (Gotoh and Patrick 1974). Utilizing both types of bars (collectively referred to as “Mn and Fe redox bars”) enables the assessment of redox classes in soils, information that is of the utmost importance because various biogeochemical processes, e.g., greenhouse gas emissions or distinct trace metal mobility, can be linked to a specific redox window. Moreover, the possibility of short-term monitoring on a weekly basis using Mn redox bars may improve the temporal delineation of soil reducing conditions, as tri- and tetravalent Mn is the preferred electron acceptor and is more easily stripped from the white PVC surface than trivalent Fe (Dorau et al. 2016). Thus far, redox bars have been successfully applied to document sulfide in marsh pore water (Rabenhorst et al. 2010), to delineate hydric soils for land classification (Castenson and Rabenhorst 2006), to visually assess the in situ formation of Fe^{III} oxides along the Mn oxide coating (Dorau et al. 2016), and further to study the sorption behavior of dissolved compounds to the remaining oxide coating (Dorau and Mansfeldt 2016). While the impact of soil temperature and E_{H} has been related to oxide removal and depletion patterns along Fe redox bars (Castenson and Rabenhorst 2006; Rabenhorst and Castenson 2005), this relationship remains unconfirmed for Mn redox bars at present. Hence, the aim of this study was to assess the impact of soil temperature and E_{H} on the reductive dissolution behavior of $\text{Mn}^{\text{III,IV}}$ and Fe^{III} oxide coatings from redox bars in water-saturated soil columns under controlled conditions in the laboratory.

2 Materials and methods

2.1 Soil sampling and soil properties

Two samples were chosen for the column experiment. First, we sampled topsoil (Ah horizon) from a floodplain soil along the Wupper River at Leichlingen, North Rhine-Westphalia,

Germany (51° 7' 10.65" N; 7° 0' 40.79" E). The soil is a Fluvisol (IUSS Working Group WRB, 2014), with sampling restricted to the humic topsoil (0 to 15 cm). Second, the loess parent material (C horizon) of a Haplic Cambisol (IUSS Working Group WRB, 2014) was sampled close to Mönchengladbach, North Rhine-Westphalia, Germany (51° 2' 58.98" N; 6° 27' 39.16" E). The two samples were selected based on their potential difference in soil organic carbon content (C_{org}) and pH. Besides the effect of temperature, sample selection accounted for the effect of variable soil properties on E_{H} development and on oxide removal along the redox bars. For a more intuitive terminology, the former soil material is hereafter referred to as topsoil and the latter as loess. Soil samples were oven-dried at 40 °C and sieved <2 mm to determine the following soil properties: soil pH, which was measured potentiometrically using a glass electrode in a 0.01 M L^{-1} CaCl_2 solution mixed 5:1 with soil (vol/vol); C_{org} , measured via dry combustion using a CNS analyzer (vario EL cube, Elementar, Hanau, Germany); grain size distribution, obtained by the sieve and settling method; and iron oxides (Fe_d), extracted using dithionite-citrate-bicarbonate (DCB). The solution was then analyzed for total iron (Fe) concentrations via flame atomic absorption spectroscopy.

2.2 Soil column experiments

The soil columns were 20 cm in length and had an inner diameter of 11.5 cm. At temperature variants of 5, 15, and 25 °C, each of the four soil columns were incubated. Two soil columns were filled to the top with topsoil and the other two with loess at a unit bulk density of 1.2 g cm^{-3} . One topsoil column was equipped with four Mn redox bars and the other topsoil column with four Fe redox bars, with the loess columns equipped with Mn and Fe redox bars in the same manner. Manganese redox bars were coated with the mineral birnessite (Dorau and Mansfeldt 2015), and the Fe redox bars with an Fe^{III} oxide suspension containing the minerals ferrihydrite and goethite (Rabenhorst et al. 2008a). The length of the bars was 22 cm (\varnothing 21 mm), with the lower 20 cm coated. Removal and re-installation of the bars took place on a weekly basis for a total period of 28 days. Briefly, the oxide removal was quantified by (i) taking a picture of each 120° redox bar section, (ii) cropping of the distorted images to an overall image, and (iii) creation of a binary image by thresholding to quantify the oxide removal into depleted and non-depleted area by using an image analysis tool (e.g., GIMP v.2.8.4). The soil columns were placed in a water bath with the water table (WT) adjusted to the middle of the soil column to facilitate reducing conditions and to separate the redox bars into an aerobic (top 100 mm) and an anaerobic part (lower 100 mm). The water bath was placed in a climate chamber (KB400, Binder, Tuttlingen, Germany) and incubated for 28 days at a temperature of 5, 15, or 25 °C. After each temperature variant, new oven-dried and sieved topsoil or loess was used to fill the soil columns, which were equipped with

newly manufactured redox bars. To determine E_H during the course of the experiments, a silver/silver chloride (Ag/AgCl) electrode (3 M KCl; SE23, Sontortech Meinsberg, Meinsberg, Germany) was placed in the center of the soil column, with platinum (Pt) tipped electrodes in duplicate at 5-, 10-, and 15-cm depth in each of the topsoil and loess columns. Soil E_H was recorded on an hourly basis for the total study period.

2.3 Assessment of mineral stability

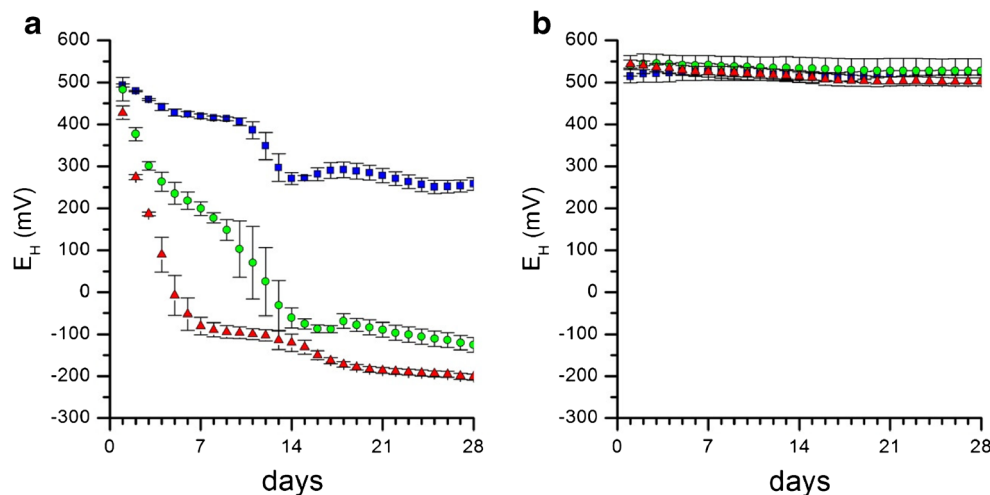
As redox reactions cause changes in soil pH, the pH of the topsoil and loess samples used in the column experiment was measured potentiometrically via a glass electrode placed in a 0.01 M L⁻¹ CaCl₂ solution mixed 5:1 with soil (vol/vol). The pH was determined exclusively at the beginning and after the incubation period of 28 days to guarantee no soil disturbance during the experiment. A linear pH change was postulated from the beginning to the end of the corresponding temperature experiment at 5, 15, and 25 °C. In this context, redox equilibrium lines can be helpful with an emphasis on predicting the stability of Mn^{III,IV} and Fe^{III} oxides (Strawn et al. 2015). If the E_H and pH of a soil are above the E_H -pH equilibrium conditions, e.g., of goethite, then ferric Fe (Fe³⁺) is in this case predicted to be the stable species. If the conditions are below equilibrium, ferrous Fe (Fe²⁺) is predicted to be the predominant species and goethite might be reductively dissolved. We used the equations for birnessite (MnO₂ + 4H⁺ + 2e⁻ = Mn²⁺ + 2H₂O; Eq. (1)), ferrihydrite (Fe(OH)₃ + 3H⁺ + e⁻ = Fe²⁺ + 3H₂O; Eq. (2)), and goethite (α-FeOOH + 3H⁺ + e⁻ = Fe²⁺ + 2H₂O; Eq. (3)) with the following Eqs. (4), (5), and (6)

$$E_H = 1290 - 118\text{pH} - 29.5 \log(c\text{Mn}^{2+}) \quad (4)$$

$$E_H = 1031 - 180\text{pH} - 59 \log(c\text{Fe}^{2+}) \quad (5)$$

$$E_H = 780 - 180\text{pH} - 59 \log(c\text{Fe}^{2+}) \quad (6)$$

Fig. 1 E_H development of soil columns packed with topsoil (a soil pH 5.8) and loess (b soil pH 7.5). Data are daily means with standard deviations of six Pt electrodes at temperatures of 5 (blue), 15 (green), and 25 °C (red)



by assuming a species concentration of either 10⁻⁶ mol Mn²⁺ or Fe²⁺ L⁻¹, 25 °C, and 0.101 MPa (Bricker 1965; Fischer 1987).

3 Results and discussion

3.1 E_H development

Figure 1 illustrates the development of E_H during the soil column experiment. Analysis of this figure reveals that the value of E_H decreased in the columns filled with topsoil from 493 to 258, 484 to -125, and from 428 to -202 mV at 5, 15, and 25 °C, respectively (Fig. 1a). In contrast, E_H remained stable at between 543 and 482 mV under all temperatures for the loess samples (Fig. 1b). We attribute this behavior to the lack of a readily available C_{org} source (electron donor), as the loess sample contained very little C_{org} (1.98 g C_{org} kg⁻¹, Table 1). Additionally, lack of adapted C-degrading microorganisms seems also reasonable as a possible explanation, since the non-fluviatile loess subsoil undergone no inundation history. On the other hand, the elevated topsoil content of 85.3 g C_{org} kg⁻¹ soil favored a decrease in E_H , even at the low temperature of 5 °C, and thus E_H development in these samples was affected with respect to temperature. As indicated by the low standard deviation and proven by the two-tailed *t* test conducted at the 5% significance level, no significant differences between Pt electrode measurements in duplicates and with monitoring depth (5, 10, and 15 cm) were recorded. Therefore, E_H development is displayed as the mean of multiple E_H measurements per soil column (Fig. 1; *n* = 6).

3.2 Mn oxide removal

The E_H -pH data for the topsoil plotted constantly below the stability line of birnessite at all temperatures (Fig. 2, Table 2).

Table 1 Selected properties of soil samples used in the column experiments

	pH	C _{org}	Sand	Silt	Clay	Fe _d
				(g kg ⁻¹)		
Topsoil	5.8	85.3	415	435	150	21.3
Loess	7.5	1.98	20	780	200	7.94

Sample pH values increased from 5.8 ± 0.01 at the beginning (Table 1) to pH 6.2 ± 0.01 (5 °C), 6.4 ± 0.02 (15 °C), and 6.6 ± 0.01 (25 °C) at the end of the incubation experiment. Equation 1 likely explains the slight increase in pH, since reduction is a proton-consuming process. In contrast, the E_H-pH values for the loess were very close and slightly below the stability line of birnessite at all temperatures (Fig. 2, Table 2), with pH values before and after the incubation experiment remaining constant at 7.5 ± 0.01 (Table 1). Hence, it can be expected that Mn^{III,IV} oxide removal from the redox bars was favorable for the topsoil but hampered for the loess. Indeed, whereas no Mn^{III,IV} oxides were removed from Mn redox bars installed in the loess (Fig. 3d–f), Mn^{III,IV} oxide removal was completed after 4 weeks of incubation at 5 °C (Fig. 3a), after 2 weeks of incubation at 15 °C (Fig. 3b), and after 1 week of incubation at 25 °C in the topsoil (Fig. 3c, Table 3). Even at a temperature of 5 °C and within a very short time frame of 7 days after water saturation, microorganisms effectively

coupled the oxidation of organic matter with the reduction of Mn^{III,IV} oxides in the topsoil, as evidenced by the partial depletion of the oxide coating (Fig. 3a, Table 3). As soil temperatures increased, Mn oxide loss was enhanced (Fig. 3b, c), with the temperature range between 5 and 15 °C and the first 7 days of activity considered to be the hot moment of Mn^{III,IV} oxides reduction, as indicated by the differences in oxide removal (Fig. 3a, b, Table 3). Overall, it has to be considered that differences in Mn oxide removal between the topsoil and loess might be also due to the absence of heterotrophic microbes and not solely a function of thermodynamic predictions of stability.

3.3 Fe oxide removal

Whereas E_H-pH data were for half of the time slightly above the stability line of ferrihydrite at 5 °C, the reductive dissolution of ferrihydrite was constantly predicted at temperatures of 15 and 25 °C in the topsoil, respectively (Fig. 2, Table 2). In contrast, the reductive dissolution of goethite was not predicted at 5 °C, because E_H-pH conditions were significantly above the stability line but predicted for 61% of the time at 15 °C and for 86% of the time at 25 °C, respectively (Fig. 2, Table 2). Although no change in color was evident for the Fe redox bars at 5 °C (Fig. 4a), a separation of the soil column into upper (above the WT) and lower parts (below the WT) became

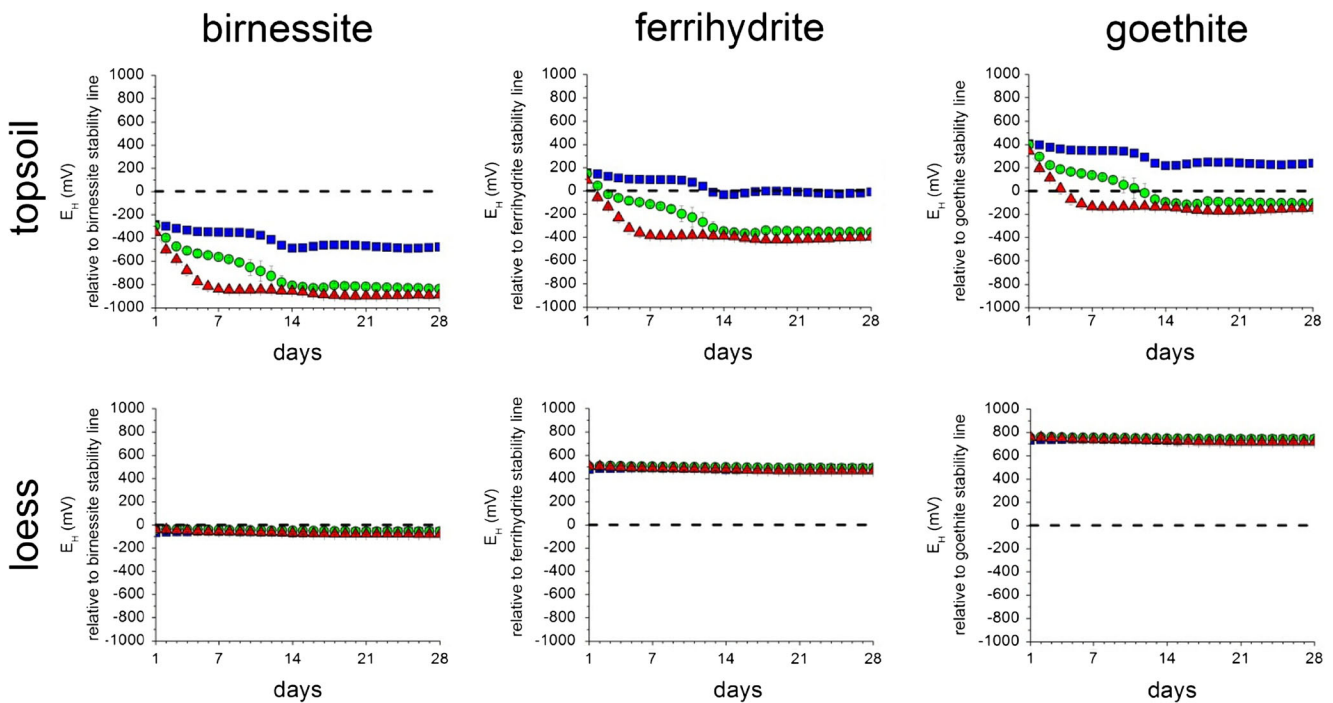


Fig. 2 E_H development as a function of time and with respect to the stability line (dashed black line in figures a to f) of birnessite, ferrihydrite, and goethite. Soil pH was determined at the beginning and at the end of the topsoil and loess column experiment and a linear pH change was employed in the stability equation. Positive values indicate no

reductive mineral dissolution and negative values indicate reductive dissolution of the designated mineral. Data are daily means with standard deviations of six Pt electrodes at temperatures of 5 (blue rectangles), 15 (green circles), and 25 °C (red triangles)

Table 2 Time period (%) the minerals employed in this study were underneath the E_H -pH stability line during the incubation experiments performed at 5, 15, and 25 °C

	Topsoil			Loess		
	Birnessite	Ferrihydrite	Goethite	Birnessite	Ferrihydrite	Goethite
5 °C	100	57	0	100	0	0
15 °C	100	93	61	100	0	0
25 °C	100	96	86	100	0	0

apparent after 2 weeks at 15 °C (Fig. 4b). As investigated by Rabenhorst et al. (2008b), the pale yellow areas present at 15 °C (Fig. 4b) and that occurred more intensively at 25 °C (Fig. 4c) reflect the preferential dissolution of ferrihydrite over goethite. This finding correlates with both the thermodynamic properties of ferrihydrite and the E_H -pH data of the incubation experiment (Figs. 2 and 4), since ferrihydrite is predicted to be removed from the PVC surface. Considering goethite removal, white PVC was not visible after 28 days but it cannot be excluded that some goethite was still removed from the bars surface (Fig. 4b, c). The appearance of the Fe redox bars installed in the loess was not altered by the removal of the oxide coating at all temperature variants (Fig. 4d–f), a result again coherent with E_H -pH data (Fig. 2).

3.4 Redox range of in situ Fe^{III} oxide formation

Even though the processes (e.g., ligand-, proton-, or electron-promoted) that lead to the dissolution of birnessite ($\log K^0$ 35.38), ferrihydrite ($\log K^0$ 3.54), and goethite ($\log K^0$ -0.02) are difficult to differentiate, organizational statements are possible, such as goethite dissolves more slowly than ferrihydrite, and Fe^{III} oxides dissolve more slowly than $Mn^{III,IV}$ oxides (Lindsay 1979; Martin 2005). This information is also valid for the constructed E_H plots (Fig. 2) and for the appearance of the oxide coating along redox bars. A number of studies have revealed that microsites in soils have an

impact on the redox milieu under both laboratory (Yang et al. 2006) and field conditions (Dorau et al. 2016). A theory that accounts for the significantly more ferrihydrite (orange color) observed here remaining along the Fe redox bar coating in the upper 0 to 10 cm compared with the lower 10 to 20 cm (Fig. 4b). However, the low standard deviation of the E_H measurements made at 5-, 10-, and 15-cm depth did not indicate any differences associated with the setting of the water table at 15 °C (Fig. 1). Hence, whereas visual differences caused by the depletion of the oxide coating enable the characterization of the soil milieu at very small scales, the equal E_H values recorded in close proximity to the artificial water table do not account for the effect of the not fully water-saturated soil pores. This has to be taken into consideration when comparing depletion patterns along redox bars with E_H measurements. Differences in oxide removal were not evident for the Mn redox bars, with no $Mn^{III,IV}$ oxide coating remaining after 28 days of installation, but less Mn oxide removal was observed from the upper part of the bars at 5 °C from day 14 to 21 (Fig. 3a–c).

Figure 5 shows a sketch of the incubation experiment, with one image of a Mn redox bar at 15 °C after 28 days of incubation. Along the artificial water table at between 9 and 10 cm (Fig. 5; see benchmark), a thin band of in situ formed Fe^{III} oxides grew from days 21 to 28 and was present at all four replicates. The origin of this band is likely the bioavailable reducible Fe^{III} oxides present in the topsoil sample at

Fig. 3 Images of Mn redox bars installed in soil columns filled with topsoil (a, b, c) and loess (d, e, f) at temperatures of 5 (a, d), 15 (b, e), and 25 °C (c, f). The removal/re-installation of redox bars took place on a weekly basis for a period of 28 days. Each image represents a composite image of three 120° sections from one bar

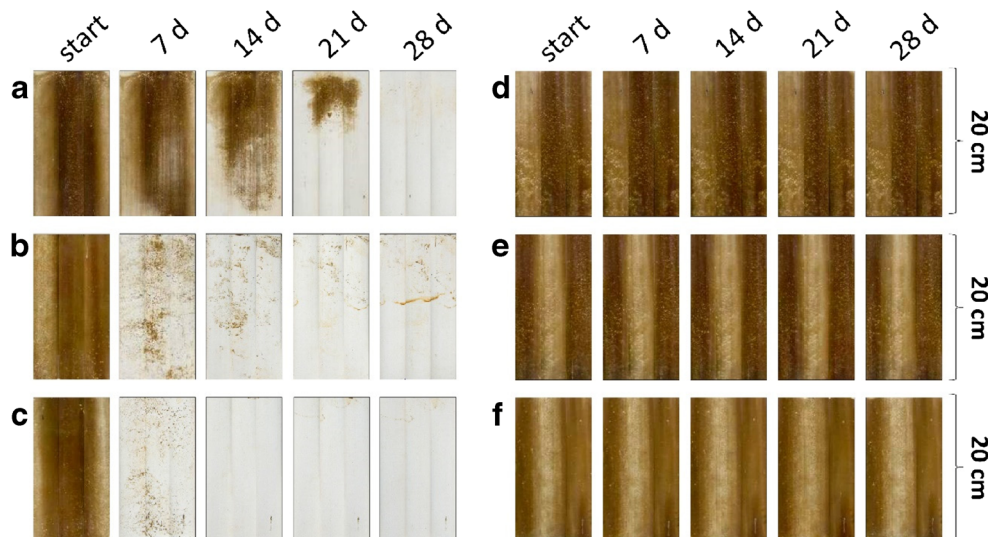


Table 3 Mean oxide removal from Mn and Fe oxide-coated redox bars installed in fourfold of the incubation experiment performed at 5, 15, and 25 °C

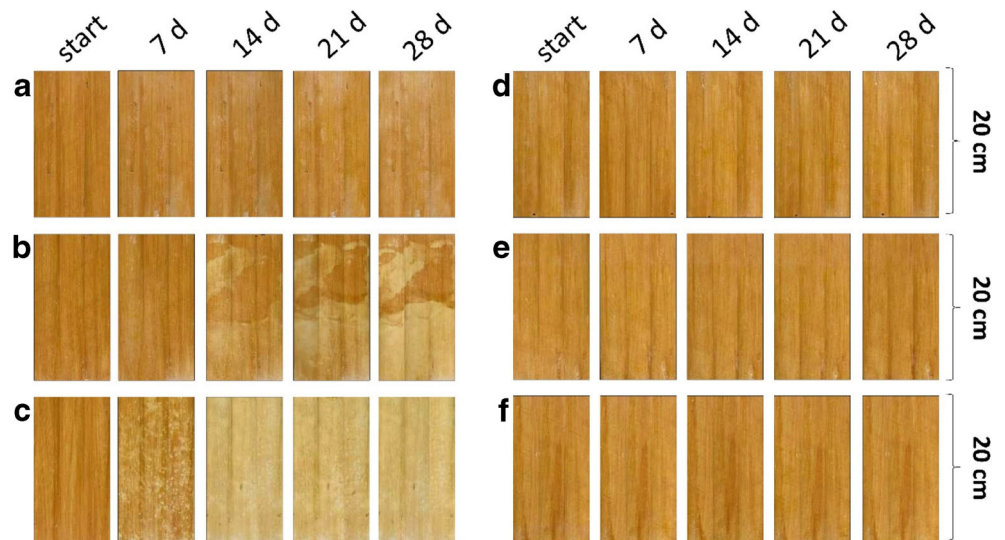
		Topsoil				Loess			
		7 days	14 days	21 days	28 days	7 days	14 days	21 days	28 days
Mn redox bar	5 °C	18 ± 4.9	56 ± 5.8	85 ± 2.7	99 ± 0.4	0.1 ± 0.1	0.1 ± 0.1	0.1 ± 0.1	0.1 ± 0.1
	15 °C	86 ± 3.1	94 ± 1.6	98 ± 0.4	100 ± 1.2	0.1 ± 0.1	0.1 ± 0.1	0.1 ± 0.1	0.1 ± 0.1
	25 °C	93 ± 1.9	99 ± 1.2	99 ± 1.0	100 ± 0.6	0.1 ± 0.1	0.1 ± 0.1	0.1 ± 0.1	0.1 ± 0.1
Fe redox bar ^a	5 °C	0.1 ± 0.1	0.1 ± 0.1	0.1 ± 0.1	0.1 ± 0.1	0.1 ± 0.1	0.1 ± 0.1	0.1 ± 0.1	0.1 ± 0.1
	15 °C	6.3 ± 4.3	58 ± 8.2	60 ± 4.9	67 ± 3.6	0.1 ± 0.1	0.1 ± 0.1	0.1 ± 0.1	0.1 ± 0.1
	25 °C	28 ± 6.7	100 ± 0.1	100 ± 0.1	100 ± 0.1	0.1 ± 0.1	0.1 ± 0.1	0.1 ± 0.1	0.1 ± 0.1

^a Percentage Fe oxide removal accounts for depletion patterns by the reductive dissolution of ferrihydrite and does not account for total Fe oxide removal

21.3 g kg⁻¹ (Table 1) that are reduced in the lower part of the soil column. This mobile ferrous Fe is translocated upwards by capillary rise and oxidizes above the artificial water table. Typically, such freshly precipitated Fe oxides are expected to be short-range ordered because of the low interfacial energies of nucleation (Stumm and Morgan, 1996). Indeed, protrusion of the Mn redox bar (Fig. 3b) into an oxalate-solution known to selectively extract short-range ordered Fe^{III} oxides from soils (Schwertmann 1964) removed the thin Fe band within minutes (data not shown), verifying the assumption of a micro-crystalline nature. Interestingly, such thin bands of Fe^{III} oxides were lacking along the Mn redox bars in the 5 and 25 °C incubation experiments because the E_H was either too high to reductively dissolve and mobilize Fe^{III} oxides (coherent with the appearance of the Fe redox bar in Fig. 4a), or too low for Fe²⁺ to be oxidized in the soil solution (Fig. 4c). Hence, there is a very narrow redox window responsible for the formation of Fe^{III} oxides, as indicated by the differences in E_H values observed from days 21 to 28 of the experiment, of -115 mV at 15 °C compared with -195 mV at 25 °C (Fig. 1a).

This has implications for the active formation of soil horizons having petrogleyic properties (e.g., bog iron; IUSS Working Group WRB 2014), which contains the following prerequisites: (i) a steady capillary rise of soil solution enriched in Fe²⁺, (ii) an O₂ barrier above the water table where Fe²⁺ is oxidized and forms Fe^{III} oxides, (iii) stable hydrologic conditions so that Fe precipitation takes place at a certain depth, and (iv) Fe enrichment then taking place over the course of centuries (Blume 1988). However, under acidic conditions, the abiotic oxidation of Fe²⁺ to Fe³⁺ by dissolved O₂ has a half-life of years (Singer and Stumm 1970), although it may be accelerated by certain bacteria in low-pH environments (Nordstrom and Southam 1997). Determination of these boundary conditions is difficult to achieve and requires both aqueous and solid phase geochemical data (Mansfeldt et al. 2012; Stanton et al. 2007). The presence of thin circumferential Fe bands along Mn redox bars, if they are frequently observed throughout annual monitoring of the soil redox milieu, might thus be an additional indicator of Fe^{III} oxide enrichment in distinct soil horizons. Manganese as an oxidant for Fe²⁺ seems to be an important precursor for the formation

Fig. 4 Images of Fe redox bars installed in soil columns filled with topsoil (a, b, c) and loess (d, e, f) at temperatures of 5 (a, d), 15 (b, e), and 25 °C (c, f). The removal/re-installation of redox bars took place on a weekly basis for a period of 28 days. Each image represents a composite image of three 120° sections from one bar



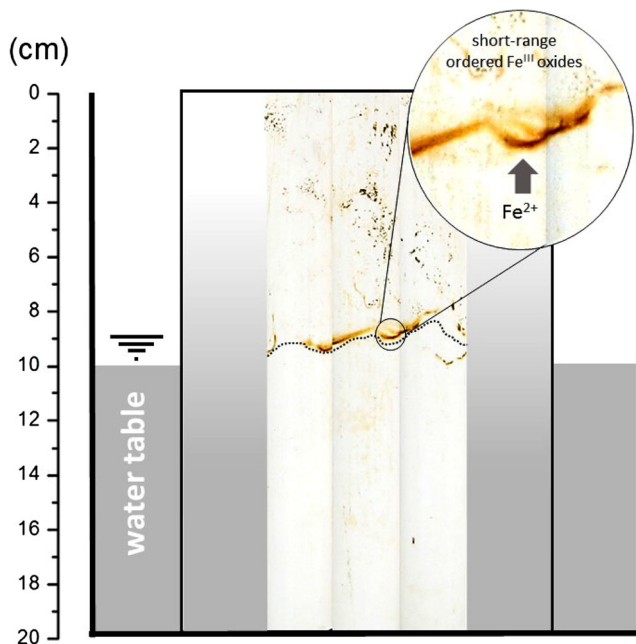


Fig. 5 Schematic drawing of soil column experiment with an example image showing one Mn redox bar after 28-day incubation in the topsoil sample at 15 °C. Note the thin band of in situ formed Fe^{III} oxides at 10-cm depth that was present in all four replicates

of durable Fe^{III} oxide coatings because these circumferential bands were barely observed along Fe redox bars (Dorau and Mansfeldt 2016). This might also relate to the fact that newly formed Fe precipitates are difficult to differentiate from the orange background of Fe^{III} oxide coatings from Fe redox bars. Apparently, Fe^{III} oxide formation along redox bars takes place under a narrow range of E_H-pH conditions. Analogous to the findings of Yu and Patrick (2004), there is also a less narrow E_H range between 180 and –150 mV where the emission of greenhouse gases is minimized (e.g., by carbon dioxide, nitrous oxide, and methane). Hence, the prevalence of a distinct redox window (spatially and temporally) has an impact on various biogeochemical processes taking place in soils. Further work is required to extend and verify the results from the laboratory experiments to field conditions.

4 Conclusions

This study demonstrated visually via the use of coated redox bars that the reductive dissolution behavior of Mn^{III,IV} oxides is strongly affected by soil temperature. At low soil temperatures of 5 °C, microorganisms were able to reduce Mn^{III,IV} oxides rapidly within a short period of days. Hence, monitoring of soil redox status on a daily basis and under moderately acidic conditions should be considered, especially in the summer when soil temperatures are high and water saturation is present. Additionally, the results obtained regarding temperature-dependent Mn^{III,IV} oxide reduction have

implications for soils affected by groundwater, perched water, flooding, and irrigation during low soil temperatures in winter, because two conditions are met in such settings: (i) water saturation prevails periodically and (ii) with generally low soil temperatures. Although the measured E_H values do not necessarily match predicted and observed Mn²⁺ or Fe²⁺ concentrations in soil solution (e.g., due to kinetic constraints and chemical non-equilibrium under natural conditions), the depletion patterns observed along the Mn and Fe redox bars are still related to E_H and pH conditions.

Acknowledgements The authors thank Mr. Roland Robel (University of Cologne, Germany) for his support and allowing the usage of facilities with which to manufacture redox bars. Dr. Gerhard Dumbeck and Mr. Manuel Endenich (both RWE POWER AG, Essen, Germany) are acknowledged for their help provided during soil sampling. We thank two anonymous reviewers for their recommendations to improve the quality of the article.

References

- Blume HP (1988) The fate of iron during soil formation in humid-temperate environments. In: Stucki JW, Goodman BA, Schwertmann U (eds) Iron in soils and clay minerals. Springer Netherlands, Dordrecht, pp 749–777
- Bricker O (1965) Some stability relations in the system Mn-O₂-H₂O at 25 °C and one atmosphere total pressure. *Am Mineral* 50:1296–1354
- Castenson KL, Rabenhorst MC (2006) Indicator of reduction in soil (IRIS): evaluation of a new approach for assessing reduced conditions in soil. *Soil Sci Soc Am J* 70:1222–1226
- Chapelle FH, McMahon PB, Dubrovsky NM, Fujii RF, Oaksford ET, Vroblesky DA (1995) Deducing the distribution of terminal electron-accepting processes in hydrologically diverse groundwater systems. *Water Resour Res* 31:359–371
- Dorau K, Eickmeier M, Mansfeldt T (2016) Comparison of manganese and iron oxide-coated redox bars for characterization of the redox status in wetland soils. *Wetlands* 36:133–144
- Dorau K, Mansfeldt T (2015) Manganese-oxide-coated redox bars as an indicator of reducing conditions in soils. *J Environ Qual* 44:696–703
- Dorau K, Mansfeldt T (2016) Manganese and iron oxide-coated redox bars as a tool to in situ study the element sorption in wet soils. *J Soils Sediments* 16:976–986
- Fiedler S, Vepraskas MJ, Richardson JL (2007) Soil redox potential: importance, field measurements, and observations. In: Sparks DL (ed) *Advances in agronomy*. Academic Press, San Diego, pp 1–54
- Fischer WR (1987) Standard potentials (E₀) of iron(III) oxides under reducing conditions. *Z Pflanz Bodenkunde* 150:286–289
- Gliński J, Stepniowski W (1985) *Soil aeration and its role for plants*. CRC Press, Boca Raton
- Goth S, Patrick WH (1972) Transformation of manganese in a waterlogged soil as affected by redox potential and pH. *Soil Sci Soc Am Pro* 36:738–742
- Goth S, Patrick WH (1974) Transformation of iron in a waterlogged soil as influenced by redox potential and pH. *Soil Sci Soc Am Pro* 38:66–71
- IUSS Working Group WRB (2014) *World reference base for soil resources 2014*. World Soil Resources Reports No. 103. FAO, Rome, Italy
- Jenkinson BJ, Franzmeier DP (2006) Development and evaluation of iron-coated tubes that indicate reduction in soils. *Soil Sci Soc Am J* 70:183–191

- Lindsay WL (1979) Chemical equilibria in soils. John Wiley & Sons, Hoboken
- Lovley DR (1991) Dissimilatory Fe(III) and Mn(IV) reduction. *Microbiol Rev* 55:259–287
- Mansfeldt T, Schuth S, Häusler W, Wagner F, Kaufhold S, Overesch M (2012) Iron oxide mineralogy and stable iron isotope composition in a Gleysol with petrogleyic properties. *J Soils Sediments* 12:97–114
- Martin ST (2005) Precipitation and dissolution of iron and manganese oxides. In: Grassian VH (ed) *Environmental catalysis*. CRC Press, Boca Raton, pp 61–81
- Nordstrom DK, Southam G (1997) Geomicrobiology of sulfide mineral oxidation. *Rev Mineral* 35:381–390
- Owens PR, Wilding LP, Miller WM, Griffin RW (2008) Using iron metal rods to infer oxygen status in seasonally saturated soils. *Catena* 73: 197–203
- Patrick WH, Gambrell RP, Faulkner SP (1996) Redox measurements of soils. In: Sparks DL (ed) *Methods of soil analysis: chemical methods part 3*. Soil Science Society of America and American Society of Agronomy, Madison, p 677
- Rabenhorst MC, Bourgault RR, James BR (2008a) Iron oxyhydroxide reduction in simulated wetland soils: effects of mineralogical composition of IRIS paints. *Soil Sci Soc Am J* 72:1838–1842
- Rabenhorst MC, Castenson KL (2005) Temperature effects on iron reduction in a hydric soil. *Soil Sci* 170:734–742
- Rabenhorst MC, Megonigal JP, Keller J (2010) Synthetic iron oxides for documenting sulfide in marsh pore water. *Soil Sci Soc Am J* 74: 1383–1388
- Rabenhorst MC, Ming DW, Morris RV, Golden DC (2008b) Synthesized iron oxides used as a tool for documenting reducing conditions in soils. *Soil Sci* 173:417–423
- Schwertmann U (1964) Differenzierung der Eisenoxide des Bodens durch Extraktion mit Ammoniumoxalat-Lösung. *Z Pflanzenemähr Düng Bodenkd* 105:194–202
- Singer PC, Stumm W (1970) Acidic mine drainage: the rate-determining step. *Science* 167:1121–1123
- Stanton MR, Yager DB, Fey DL, Wright WG (2007) Formation and geochemical significance of iron bog deposits. US Geological Survey, Washington
- Strawn DG, Bohn HL, O'Connor GA (2015) *Soil chemistry*, fourth edn. John Wiley & Sons, Hoboken
- Stumm W, Morgan JJ (1996) *Aquatic chemistry*, third edn. Wiley, New York
- Yang J, Hu Y, Bu R (2006) Microscale spatial variability of redox potential in surface soil. *Soil Sci* 171:747–753
- Yu KW, Patrick WH (2004) Redox window with minimum global warming potential contribution from rice soils. *Soil Sci Soc Am J* 68:2086–2091